euspen's 24th International Conference & Exhibition, Dublin, IE, June 2024
www.euspen.eu

Effect of electric fields on micro-scratching of calcium fluoride

Yunfa Guo[1], Jiaming Zhan[1]

[1]*Department of Mechanical Engineering, College of Design and Engineering, National University of Singapore*

guo.yunfa@u.nus.edu

Abstract

Electric field assistance has shown positive effectiveness in facilitating the machining of conductive materials (e.g., metals and alloys). However, the electric field effect on the manufacturing performance of non-conductive materials is less studied. In this study, an external electric field is employed in micro-scratching of a non-conductive ceramic material, single-crystal calcium fluoride (CaF_2). The electric field effect on the machinability of non-conductive CaF_2 was assessed by characterizing scratched surface morphology, critical load, scratch profile, and acoustic emission (AE) signals. Compared to conventional scratching, the scratched surface quality was improved with fewer cracks and surface defects after applying the electric field. The critical load that quantitatively identifies the position of ductile-brittle transition and crack formation was larger with the electric field. A smoother cross-sectional scratch profile and larger residual depth were observed with the assistance of an electric field. The lower AE amplitude with the electric field further suggests that the application of the electric field can effectively suppress brittle material removal of single-crystal CaF_2 in micro-scratching. The mechanism responsible for enhanced machinability of CaF_2 in the presence of an electric field was discussed based on the theory of electro-plasticity and further revealed by molecular dynamics simulations. This study deepens the comprehension of electric field-assisted machining technology in non-conductive materials and opens a novel path for improving the manufacturing efficiency of ceramic components.

Keywords: electric field, non-conductive materials, calcium fluoride, machinability, micro-scratching

1. Introduction

The machining efficiency is significantly influenced by the unique properties of workpiece materials, such as excessive plastic deformation in ductile metals [1,2] or high brittleness in ceramics and glasses [3,4]. These distinct material characteristics impose significant limitations on the machinability of materials with specific properties, hampering their broader application. Physical field-assisted machining provides a way to augment the machinability of difficult-to-machine materials by inducing targeted modifications in material properties and deformation behaviours. Typical physical fields employed in machining include electric field [5], magnetic field [6,7], and thermal field [8,9]. Compared to thermal field assistance, electric field and magnetic field can be readily implemented and controlled in existing machine tools, contributing to both improved processing revenue and a more environmentally friendly machining environment. In this paper, we conducted an original investigation to estimate the effectiveness of electric field assistance in micro-scratching of non-conductive ceramic material.

Electric field assistance has been successfully employed in various manufacturing processes for conductive metal alloys, which include wire drawing [10], sheet forming [11], sintering [12], forging [13], material joining [14], and rolling [15]. Positive improvements were observed in these manufacturing processes, e.g., reduction in forming and cutting forces, weakened elastic recovery, quicker ageing and recrystallization, increased formability, and lower specific energy for deformation. However, the advantages of electric field assistance have not been fully harnessed in the machining of non-conductive ceramics, let alone in the realm of precision micro-scratching. Furthermore, the thermal effects induced by electric current, such as joule heating, thermal softening, and thermal expansion, continue to be significant considerations in the study of conductive materials [16]. The existence of thermal effect makes it challenging to ascertain the role of the electric effect in the improvement of machining performance during machining of metals and alloys.

The literature on the positive impact of the electric field on conductive materials offers a potential application for the assistance of the electric field to enhance the machinability of non-conductive ceramics. Therefore, load-varying micro-scratching tests with and without the assistance of an electric field were performed in this paper. This work focuses on the influence of an electric field on non-conductive calcium fluoride (CaF_2) crystal during the scratching process, which is unlikely to involve thermal effects that potentially affect the results of the investigation. The electric field effect on the machinability of non-conductive CaF_2 crystal was assessed by characterizing scratched surface morphology, critical load, scratch profile, and acoustic emission (AE) signals. Subsequently, the material removal mechanism in electric field-assisted scratching of non-conductive CaF_2 was uncovered by the electro-plasticity theory and molecular dynamics (MD) simulations.

2. Methodology

2.1. Micro-scratching tests with electric field

Micro-scratching tests were carried out on an Anton Paar Step 300 - MCT³ Micro Combi Tester, as shown in Figure 1. A non-conductive ceramic material, (111) single-crystal CaF_2, was chosen as the case material to eliminate the thermal effects. The sample of (111) CaF_2 crystal was purchased from Latech Singapore with dimensions of $10\ \text{mm} \times 10\ \text{mm} \times 2\ \text{mm}$. Load-

varying micro-scratching tests, with and without the assistance of an electric field, were performed using a Rockwell indenter with a 100 µm radius. During scratching, the applied normal force increased linearly from 0.03 N to 1 N over a length of 1 mm, with a constant speed of 10 mm/min. The scratching direction was along the $[11\bar{2}]$ crystallographic orientation of (111) CaF_2 crystal. A direct current (DC) power source generated the electric field, with an intensity set at 10 V/cm and aligned with the scratching direction.

Scratched surface morphology and scratch profiles were analyzed using the Olympus LEXT OLS5500 laser confocal microscope. The critical normal load, indicating the position of the ductile-brittle transition and the initiation of the first crack, was determined using integrated analysis software in the Micro Combi Tester. Additionally, AE signals during the scratching process were recorded with an AE sensor integrated into the Micro Combi Tester.

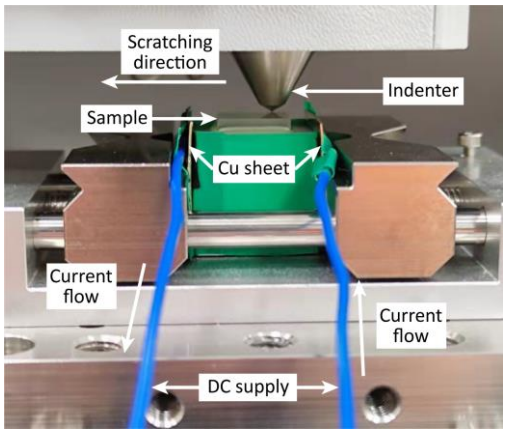

Figure 1. Electric field-assisted micro-scratching setup.

2.2. Molecular dynamics simulations

MD scratching simulation with the influence of electric field was conducted on CaF_2 crystal using the Large-scale Atomic/Molecular Massively Parallel Simulator (LAMMPS). Figure 2 displays the MD simulated scratching model of CaF_2 with a dimension of $50\ \text{nm} \times 23\ \text{nm} \times 13\ \text{mm}$ along $[11\bar{2}]$, $[\bar{1}10]$, and $[111]$ directions, respectively. The diamond indenter (spherical cap with a 12 nm radius of sphere) first penetrated the (111) surface of CaF_2 crystal. After the penetration depth reached 0.7 nm, the indenter maintained the depth for scratching along $[11\bar{2}]$ direction with a constant speed of 100 m/s over a distance of 30 nm. During MD simulations, the Buckingham interatomic potential and Lennard-Jones potential [17,18] were respectively used to model the workpiece atom interaction and indenter-workpiece interaction. The external electric field was applied in MD simulated scratching in the form of Coulomb force ($F = qE$). In MD simulations, the electric field intensity and direction were defined as 1 V/nm and aligned parallel to the scratching direction. The discrepancy in electric field intensity between MD simulations and experimental results is attributed to the size effect and geometric factors [17].

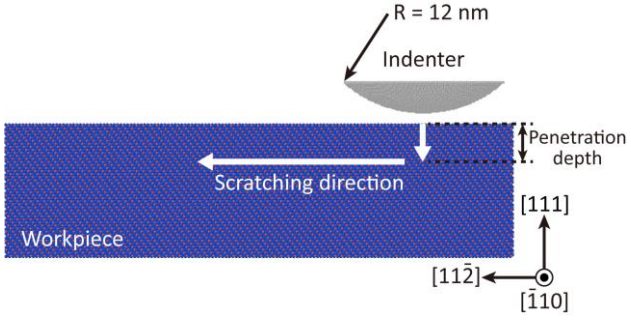

Figure 2. MD simulated model of scratching of CaF_2 crystal.

3. Results

3.1. Scratched surface morphology

Figure 3 shows the scratched surface morphology of CaF_2 crystal without and with the assistance of an electric field. The scratched surface was firstly covered with a damage-free region, i.e., ductile-removal region. With increasing normal load, defects and cracks started to appear on the scratched surface, i.e., the brittle-removal region. The brittle-removal region without the assistance of an electric field exhibited three types of defects: material peeling, lateral crack, and radial crack. It can be seen from Figure 3 that the application of the electric field enlarged the range of the ductile-removal region and delayed the crack formation (especially the material peeling) during the brittle-removal region.

As displayed in Table 1, the application of the electric field also increased the critical load for ductile-brittle transition and the first crack formation in micro-scratching of CaF_2 crystal. The critical load for the transiting point of the ductile-brittle region showed an increase of 52%, ranging from 630 mN without an electric field to 958 mN with the electric field. The critical load for the initial lateral crack rose from 949 mN to 958 mN with the introduction of an electric field. Similarly, the application of an electric field resulted in an escalation of the critical load for the first radial crack, increasing from 974 mN to 1000 mN. These results quantitatively indicate that electric field-assisted machining can significantly enhance the machining efficiency in achieving damage-free surfaces during micro-scratching of non-conductive brittle ceramics.

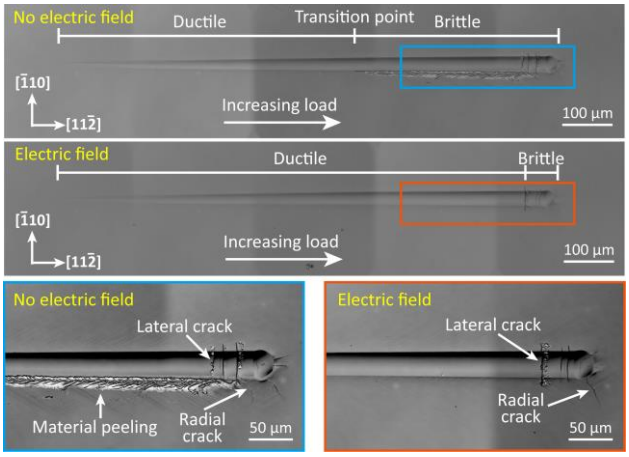

Figure 3. Scratched surface morphology without and with electric field.

Table 1 Critical load (mN) for ductile-brittle transition and the first crack formation without and with electric field.

Position	Critical load (mN)	
	No electric field	Electric field
Ductile-brittle transition	630 mN	958 mN
The first lateral crack	949 mN	958 mN
The first radial crack	974 mN	1000 mN

3.2. Scratch profile

Figure 4(a) presents the height image of residual scratch after micro-scratching under no electric field and electric field. As shown in Figure 4(a), cross-sectional scratch profiles were measured at three positions with different normal loads (400, 630, 900 mN), which respectively represent the positions of ductile removal, ductile-brittle transition, and brittle removal at electric-free condition. Figure 4(b) shows the distribution of cross-sectional scratch profile at three different normal loads without and with electric field. At the position with the applied load of 400 mN, smooth scratch profiles were observed

regardless of electric field conditions. When the applied normal load increased to 630 mN, the scratch profile without an electric field showed significant fluctuation at one side, which is attributed to the material peeling on the scratched surface. The fluctuation of the scratch profile at electric-free conditions increased at the higher normal load (900 mN). Conversely, the cross-sectional scratch at all three normal loads exhibited a smooth and stable profile with the electric field. The residual depth is an indicator of the plastic deformation degree. As recorded in Table 2, the cross-sectional residual depth increased with the electric field at all three normal loads. It suggests that the application of an electric field can augment the plastic deformation of CaF_2 crystal.

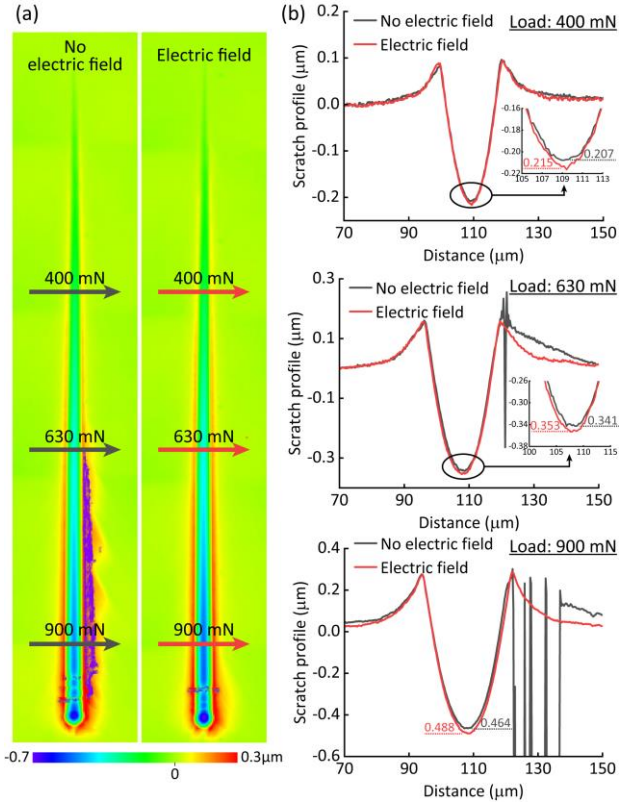

Figure 4. Scratch profile without and with electric field.

Table 2 Residual depth (μm) without and with electric field.

Applied normal load (mN)	Residual depth (μm)	
	No electric field	Electric field
400	0.207	0.215
630	0.341	0.353
900	0.464	0.488

3.3. *Acoustic emission signals*

The AE sensor is capable of capturing signals corresponding to the energy dissipated during the generation of a new surface, as defects and cracks form on both the surface and subsurface during micro-scratching [19]. Therefore, the amplitude of the recorded AE signals reveals the degree of crack formation in micro-scratching. Figure 5 illustrates the recorded AE waveforms without and with electric fields. The percentage of AE voltage in Figure 5 was determined by computing the ratio of the measured voltage to the fixed electronic circuit voltage within the AE sensor system, reflecting the amplitude of AE signals. As illustrated in Figure 5, the introduction of an electric field resulted in a reduction in AE amplitude (AE voltage). It further indicates that the electric field assistance can suppress crack formation and brittle material removal during micro-scratching of CaF_2 crystal.

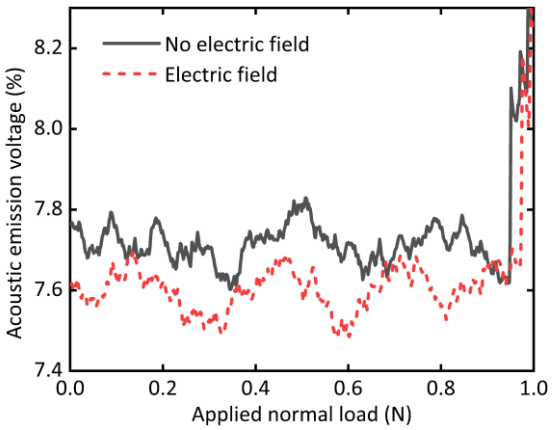

Figure 5. Acoustic emission waveforms during scratching without and with electric field.

4. Material removal mechanism

4.1. Electro-plastic effect

The ductile removal of crystalline ceramics in micro-scratching is governed by dislocation-dependent plastic deformation. Hence, the observed extension in the ductile removal region during scratching of CaF_2 crystal is believed to result from enhanced dislocation plasticity under an electric field. According to Conrad [20], the application of an electric field has shown a favourable potential to increase the plasticity of materials, even in non-conductive ceramics, which is defined as the electro-plastic effect or electro-plasticity. Two potential scenarios were used to expound the electro-plastic effect on dislocation plasticity [20]. On one hand, the application of an external electric field induces a force on charged dislocations via electrostatic Coulomb interaction. This, in turn, enhances the mobility of dislocations, enabling them to surmount obstacles that impede deformation. On the other hand, as illustrated in Figure 6, charged barrier-dislocation radical pairs can also be reoriented to a uniform orientation where the radical pairs transit from singlet state to triplet state under an electric field, which would lower the pinning force between barriers and dislocations to decrease the resistance for dislocation motion. As a result, improved dislocation motion under an electric field promotes plastic deformation, which further lowers stress concentration and suppresses crack formation for extending the ductile removal region and increasing the ductile-brittle transition in scratching of CaF_2 crystal. The results of MD simulations discussed in the next section will be employed to confirm the theory of electro-plasticity.

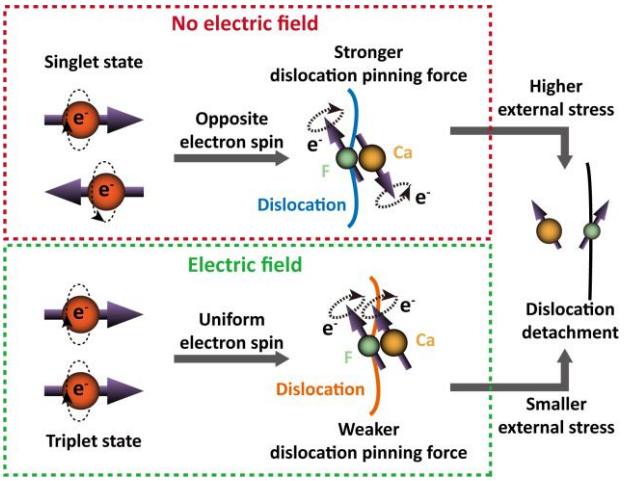

Figure 6. Enhanced dislocation movement due to the spin conversion of charged barrier-dislocation radical pairs under an electric field.

4.2. *MD simulated material removal behaviours*

Figure 7 presents the influence of the electric field on dislocation distribution at different scratching distances. During MD simulated scratching, dislocations mainly propagated along the penetration direction and scratching direction, which is governed by the primary dislocation slip systems {100} <110> of CaF_2 crystal [21]. The application of the electric field had a slight effect on the direction of dislocation propagation. Oppositely, the dislocation distribution range is significantly affected by the applied electric field. It is evident in Figure 7 that a larger range of dislocation distribution was observed during scratching with the assistance of an electric field. The result suggests that the applied electric field can promote the dislocation movement and plastic deformation of CaF_2 crystal. In addition, the total dislocation line length was also measured in Figure 8. The dislocation line length increased with increasing scratching distance regardless of electric field conditions, which is attributed to dislocation accumulation with new dislocation formation during scratching. Compared to the electric-free condition, the applied electric field increased the length of dislocation lines during the total scratching process, which reconfirms the enhanced plasticity with an electric field.

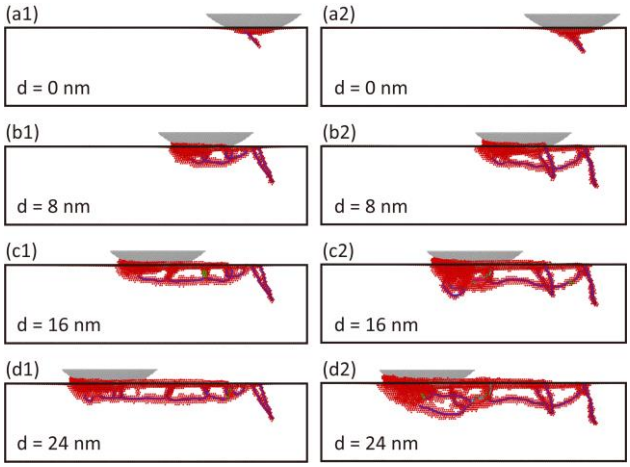

Figure 7. Representative MD snapshots of dislocation distribution at different scratching distances without electric field (a1-d1) and with electric field (a2-d2). The letter 'd' represents the scratching distance.

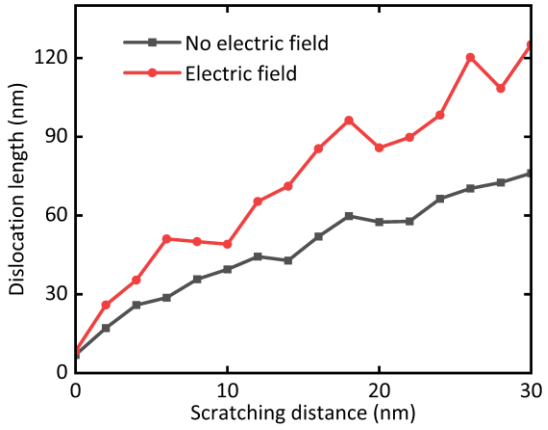

Figure 8. Dislocation line length during scratching without and with the electric field.

5. Conclusions

In this work, electric field-assisted micro-scratching tests and MD simulations were conducted to investigate the potential of electric field to enhance the machinability of a non-conductive ceramic material, single-crystal CaF_2. The contributions of this study are highlighted as follows:

(1) The application of electric field can result in a substantial reduction in surface damage and up to a 50% increase in damage-free machining load (i.e., ductile-brittle transition load) in micro-scratching of non-conductive CaF_2 crystal.

(2) The increased residual depth under the influence of an electric field signifies heightened plastic deformation in the CaF_2 crystal. The reduced AE amplitude with electric field suggests suppressed brittle fracture of CaF_2 crystal in micro-scratching.

(3) Based on the electro-plastic effect, electric field assistance facilitates the machinability of CaF_2 crystal by the electric field acting as a mediator that improves dislocation mobility through the Coulomb interaction and spin conversion.

(4) MD simulated scratching of CaF_2 crystal showed a broader distribution of dislocations and an augmented length of dislocation lines after applying the electric field. It provides additional support for the theory of enhanced dislocation mobility under the electric field effect (i.e., electro-plasticity).

The experimental and theoretical studies of the electric field effect on scratching of non-conductive CaF_2 crystal will provide guidelines for better design and development of precision machine tools equipped with a well-designed electric field environment for the efficient manufacturing of ceramics.

Acknowledgements

This research was supported by the Singapore Ministry of Education Academic Research Funds (Grant Nos.: MOE-T2EP50120-0010, MOE-T2EP50220-0010, and A-8001225-00-00). We thank the guidance of Dr Hao Wang at the Department of Mechanical Engineering, National University of Singapore (email: mpewhao@nus.edu.sg).

References

[1] Guo Y, Lee YJ, Zhang Y and Wang H 2022 *J. Mater. Sci. Technol.* **124** 121–134
[2] Chaudhari A, Soh ZY, Wang H and Kumar AS 2018 *Int. J. Mach. Tools Manuf.* **133** 47–60
[3] Guo Y, Lee YJ, Zhang Y, Sorkin A, Manzhos S and Wang H 2022 *J. Mater. Sci. Technol.* **112** 96–113
[4] Lee YJ, Kumar AS and Wang H 2021 *Int. J. Mach. Tools Manuf.* **168** 103787
[5] Bilal A, Jahan M, Talamona D and Perveen A 2018 *Micromachines* **10** 10
[6] Guo Y, Zhan J, Lee YJ, Lu WF and Wang H 2023 *Int. J. Mech. Sci.* **249** 108272
[7] Guo Y, Zhan J, Lu WF and Wang H 2024 *Int. J. Mech. Sci.* **263** 108768
[8] Wang H, Senthil Kumar A and Riemer O 2018 *Proc. Inst. Mech. Eng. Part B J. Eng. Manuf.* **232** 1123–1129
[9] Chua J, Zhang R, Chaudhari A, Vachhani SJ, Kumar AS, Tu Q and Wang H 2019 *Int. J. Mech. Sci*. **159** 459–466
[10] Tang G, Zhang J, Yan Y, Zhou H and Fang W 2003 *J. Mater. Process. Technol.* **137** 96–99
[11] Fan G, Gao L, Hussain G and Wu Z 2008 *Int. J. Mach. Tools Manuf.* **48** 1688–1692
[12] Langer J, Hoffmann MJ and Guillon O 2009 *Acta Mater.* **57** 5454–5465
[13] Jones JJ, Mears L and Roth JT 2012 *J. Manuf. Sci. Eng.* **134**
[14] Skovron JD, Ruszkiewicz BJ, Mears L and Abke T 2016 *Proceedings of the ASME 11th International Manufacturing Science and Engineering Conference*
[15] Li X, Wang F, Li X, Zhu J and Tang G 2017 *Mater. Sci. Technol.* **33** 215–219
[16] Dimitrov NK, Liu Y and Horstemeyer MF 2020 *Mech. Adv. Mater. Struct.* **29** 705–716
[17] Zhan J, Guo Y and Wang H 2024 *Int. J. Mech. Sci.* **261** 108693
[18] Zhan J, Guo Y and Wang H 2024 *J. Eur. Ceram. Soc.* **44** 1795–1805
[19] Gu X, Zhao Q, Zhang J, Guo B and Wang H 2020 *Ceram. Int.* **46** 26085–26099
[20] Conrad H 2000 *Mater. Sci. Eng. A* **287** 276–287
[21] Wang H, Riemer O, Rickens K and Brinksmeier E 2016 *Scr. Mater.* **114** 21–26